New Methodologies for Measuring Film Thickness, Coverage, and Topography

C. Mathew Mate, Bing K. Yen, Dolores C. Miller, Mike F. Toney, Mike Scarpulla, and Jane E. Frommer

***Abstract*—We describe how the techniques of X-ray reflectivity (XRR), electron spectroscopy for chemical analysis (ESCA), and atomic force microscopy (AFM) can be used to obtain the structural parameters—thickness, coverage, and topography—of thin films used on magnetic recording disks. We focus on ultra-thin amorphous nitrogenated carbon (CNx) overcoats on disks. Each technique has its own strengths: XRR measures film thickness absolutely, ESCA determines the chemical composition of the films, and AFM maps topography accurately. For the CNx overcoats investigated, we find incomplete coverage for thicknesses less than 20 Å, and we find a small surface roughness with rms roughness $\leq$ 11 Å.**

***Index Terms*—Atomic force microscopy, electron spectroscopy for chemical anylsis, thin films, X-ray reflectivity.**

I. Introduction

INCREASING the density of information stored within disk drives by scaling methods has lead to smaller dimensions for components and features within drives. For example, to protect the magnetic media from sliding contacts with the recording head, disks inside drives typically have carbon overcoats less than 100 Å in thickness and covered with about 10 Å of lubricant. These films also have to protect the underlying magnetic layer from corrosion. Within a few years, the combined thickness of the overcoat and lubricant is expected to be less than 50 Å, and the individual thicknesses will need to be controlled to much better than a nanometer. Similarly, surface topographies of disks and sliders are becoming smoother with the rms roughness approaching atomic dimensions. These trends require that the disk drive industry answer two key questions in the next several years:

- How will it measure accurately the small thicknesses and topography variations for these thin films?
- What limits how thin a film, like the carbon overcoat, can be made and still provide adequate tribological protection? Similarly, what limits how smooth a disk surface can be made?

In this paper, we show that, by combining the attributes of various measurement techniques, one can accurately measure the structural parameters of thickness, coverage, and topography of carbon overcoats only a few nanometers in thickness on disk surfaces. The techniques used in this study and their relative merits are:

- *X-ray reflectivity (XRR)* provides absolute measurement of film thickness and rms roughness.
- *Electron spectroscopy for chemical analysis (ESCA)* provides elemental chemical composition and, if an appropriate model is used, film thickness.
- *Atomic force microscopy (AFM)* provides an accurate map of topography.

For a series of nitrogenated carbon (CNx) overcoats used in this study, we find that

- Their *thickness* can be accurately measured using either XRR or ESCA, when calibrated by XRR.
- ESCA detects the formation of a metal oxide layer for overcoat thickness less than 20 Å. We use the ESCA thickness of this oxide layer as a measure of the *coverage* of the carbon overcoat. The results suggest that about 20 Å may represent the limit as to how thin a carbon overcoat can be made using conventional sputter deposition processes and still provide adequate protection of the underlying magnetic layer.
- AFM and XRR both indicate that *topography* variations increase with increasing CNx overcoat thickness. For all the overcoat thickness studied (up to 50 Å), the rms roughness is $\leq$ 11 Å, showing that, for a smooth substrate on which a simple film structure is deposited, the roughness of the top surface of a disk can be made within a factor of ten of atomic dimensions.

II. Experimental

A. Thin Film Disk Preparation

To provide an optimum structure for the XRR measurements, it is desirable to start with the smoothest possible substrate and to have a film structure with the least number of layers. Consequently, our thin film disk structure differs from a conventional structure: First, glass substrates are selected for their high degree of smoothness over short lateral length scales (<2 μm). Second, the magnetic layer (a quaternary cobalt alloy) is sputter-deposited directly onto the glass substrate without any underlayer. On top of the magnetic layer, an amorphous nitrogenated carbon (CNx) overcoat is sputter-deposited to different thicknesses by varying the sputtering time. The results reported here are for unlubricated surfaces; our results for lubricated surfaces are discussed elsewhere [1], [2].

Manuscript received July 23, 1999. M. Scarpulla was supported to work at IBM Almaden by NSF Grant 9300131.

C. M. Mate, B. K. Yen, D. C. Miller, M. F. Toney, and J. E. Frommer are with the IBM Research Division, Almaden Research Center, San Jose, CA 95120 (e-mail: {mate; bkyen; dcmiller; toney; frommer}@ almaden.ibm.com).

M. Scarpulla's present address is the Materials Science Department, Brown University, Providence, RI 02912 (e-mail: scarps1@yahoo.com).

Publisher Item Identifier S 0018-9464(00)00267-3.

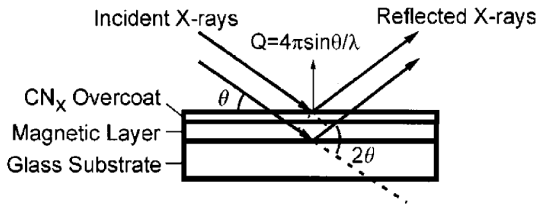

Fig. 1. Thin film structure and X-ray reflectivity geometry.

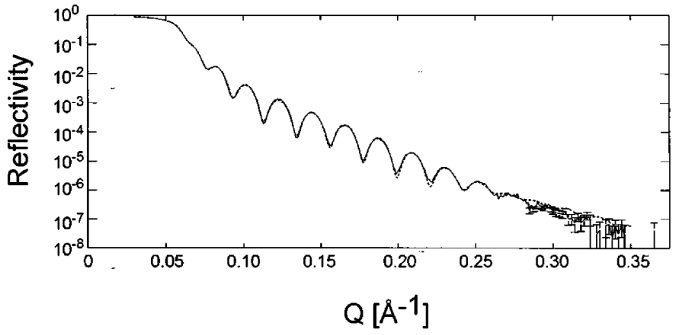

Fig. 2. X-ray reflectivity from a typical disk structure. Solid line follows the measured values, and the dotted line follows the calculated values using the best fit model.

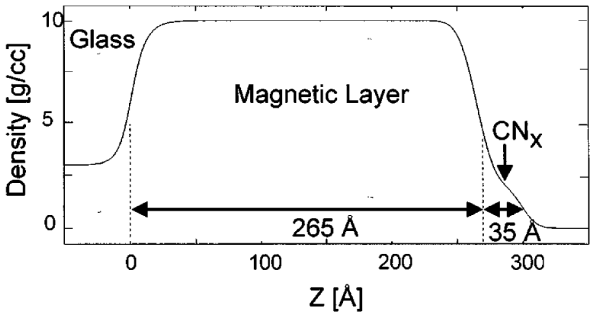

Fig. 3. Mass density profile, including interface broadening and roughness, for a thin film disk structure calculated from the best fit shown in Fig. 2.

B. Techniques

1) X-Ray Reflectivity (XRR): The geometry for low-angle X-ray reflectivity is illustrated in Fig. 1. X-rays impinge on the sample at a small angle θ, and the intensity of the specularly reflected X-rays is detected at 2θ. The reflected intensity is measured as a function of θ, normalized by dividing by the incidence intensity, and plotted as a function of $Q = 4\pi \sin\theta/\lambda$. The XRR experiments are conducted using Cu K_{a1} radiation ($\lambda = 1.542$ Å) from an 18 kW X-ray generator. The beam size at the sample is defined by slits: In the scattering plane, the slit width is 0.05 mm for $Q > 0.15$ Å^{-1} and 0.12 mm for $Q > 0.15$ Å^{-1}. Out of the scattering plane, the slit width is 4.0 mm. The angular acceptance of the detector, also defined by slits, is 1.75 milliradian (mrad) in the scattering plane and 20 mrad out of the scattering plane. The background (diffuse) scattering is subtracted from the raw data to yield the true specular reflectivity [3], [4]. The coherence length for this instrument is about 2 μm [5], meaning that the measured roughness is averaged over lateral length scales from 1 Å to 2 μm.

The specular reflectivity of X-rays is analogous to optical reflectivity [3], [4], [6]. At X-ray energies, the refractive index n is slightly less than unity, and $1 - n$ proportional to electron density. At film interfaces, the electron density, and hence n, changes, causing some of the X-rays to be reflected at the interfaces. Since a film always has top and bottom interfaces, interference between X-rays reflected at these interfaces leads to an oscillatory pattern, akin to optical interference fringes, with the oscillation period inversely proportional to the film thickness. The decay in oscillation amplitude with increasing Q is related to the interfacial roughness with higher roughness causing a faster decrease in the oscillation amplitude. So long as the film thickness is larger than its interfacial width or roughness, the film thickness can be determined directly from the fringe spacing, although a more sophisticated modeling discussed below is also used to analyze the data.

Fig. 2 shows an example of the data collected from a disk structure illustrated in Fig. 1. For incident angles less than some critical value, the incident X-ray beam is totally reflected. Above this critical angle, the reflectivity drops quickly, but the oscillations from interference within the thin film structure are clearly visible. The dominant oscillations have a period of $\Delta Q = 0.024$ Å^{-1}, corresponding to interference within the magnetic film, which has a thickness $d = 2\pi/\Delta Q = 265$ Å. These short period oscillations are modulated by another oscillation with a much longer period ($\Delta Q = 0.18$ Å^{-1}) from interference within the thin carbon overcoat.

To analyze the XRR data more quantitatively, we use a multilayer model analogous to that employed in standard optics (Fresnel formulae) [3], [4], [6]. The model incorporates several variable parameters—film thickness, density, and roughness of each film and interface—which are fitted to the data. For any interface, the roughness can take many forms, but a Gaussian roughness distribution (error function density profile) is typically assumed. The dotted line in Fig. 2 shows the best fit model for that data set and matches almost exactly with the solid data line. The best fit to the data was determined from the minimum χ^2 [2]-[4], which is typically 5–10 for the best fits. The error bars on the data are the (quadratic) sum of the statistical errors and 0.02 times the reflectivity.

The quality of the fit in Fig. 2 is superior to what could be achieved for a conventional disk from a disk drive, as the smoother substrate and films make the interference oscillations extend to higher Q and the smaller number of films greatly reduces the number of parameters to be fitted in the model.

Fig. 3 shows the density profile determined by this best fit for the data in Fig. 2. Even though the CNx overcoat is a very thin film sitting on a much thicker magnetic layer, XRR is still able to determine its thickness unambiguously. In addition to film thickness and electron density, XRR is also able to determine the rms interface widths (± 0.5 Å) in the disk structure: 6.7 Å for glass/mag, 10.9 Å for mag/CNx, and 8.7 Å for CNx/air for the example in Fig. 2. Thus, using a smooth glass substrate (5–7 Å rms roughness for the initial glass/air interface) and a simplified disk structure, a top surface with < 10 Å roughness is obtained, which is also confirmed by AFM. We will discuss this point further later in the paper.

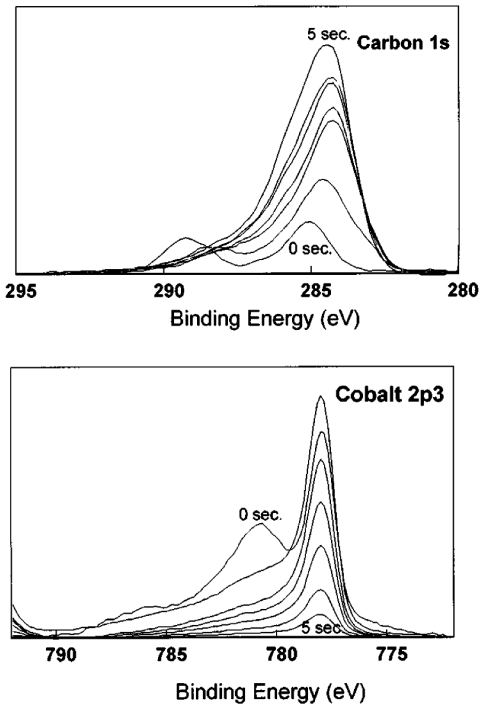

Fig. 4. ESCA intensity for the C1s and Co2p3 core levels for the following CNx sputtering times: 0, 1, 1.5, 2, 2.5, 3, and 5 s.

2) Electron Spectroscopy for Chemical Analysis (ESCA): The ESCA data are taken with a Surface Science SSX-100 spectrometer using monochromatized Al K_α X-rays. Core level peaks of the following elements are collected at an exit angle of $\Theta = 37°$: Co, Pt, Cr, O, C, and N. Fig. 4 shows how the intensities of the C1s and the Co2p3 core levels vary with the deposition time for the CNx overcoat. From the figure, one sees that, as expected, the cobalt signal decreases (because of attenuation by the growing overcoat) as the carbon signal increases with increasing overcoat deposition time. One also sees for short deposition times (i.e., little or no overcoat) a strong Co2p3 peak at higher binding energy, indicating cobalt oxide forming when the overcoat is very thin. Later, we discuss how this and the other metal oxide ESCA peaks are used to determine the coverage of the CNx overcoat. Even when no overcoat is deposited, a carbon signal is still present in the C1s signal, presumably from hydrocarbon contaminants adsorbing onto the magnetic layer after the disk is removed from the sputtering system.

Using the intensities of ESCA core level peaks, we can determine the thicknesses of the overcoat and metal oxide layers by using a single-mean-free-path model [1], [2], [7]. In this model, the electron mean-free-path λ_e is assumed to be the same for all materials in the thin film structure and independent of the electron kinetic energy. The film thicknesses are then calculated using Beer's law of attenuation of underlayer signals by overlying layers. For example, the signal I_o originating from the magnetic layer would be attenuated by the overcoat of thickness d according to the relationship: $I = I_o \exp(-d/\lambda_e \sin\Theta)$. Within this model, we further assume that I = (sum of the percents of the ESCA signals from the underlayer elements) and I_o = (sum of underlayer and overlayer percents). We assume the multilayer structure shown in Fig. 5 for the analysis, where various layers are assumed to be ideally smooth and continuous and the interfaces to be abrupt.

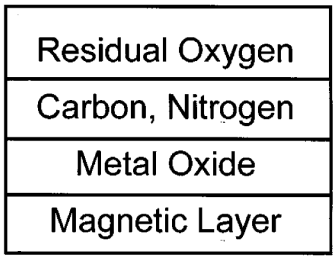

Fig. 5. Film structure assumed for analyzing the ESCA data.

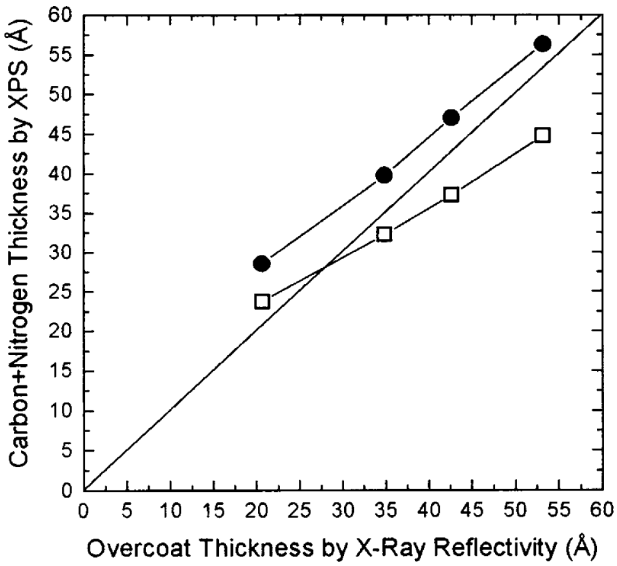

Fig. 6. Comparison of the overcoat thickness as determined by ESCA and XRR assuming either λ_e = 15 Å (open squares) or λ_e = 20 Å (closed circles).

3) Atomic Force Microscopy (AFM): AFM images are collected on a commercial, large-stage instrument with laser deflection detection. Intermittent contact mode is used with triangular tungsten-carbide coated silicon cantilevers, 110 μm long and ~120 kHz resonance frequency. The rms roughness is determined with the algorithms provided by the instrument manufacturer's operating software and is based on the standard deviation of the z-values (heights) over a 256 × 256 matrix of data points of a 2.0 μm × 2.0 μm area.

III. Results for Nitrogenated Carbon Overcoats

A. ESCA and XRR Thickness Comparison

Fig. 6 shows how the overcoat thickness determined by ESCA using the single-mean-free-path model compares with the overcoat thickness determined by XRR assuming either λ_e = 15 or 20 Å. Both mean-free-paths determine ESCA thicknesses that agree to within 20% with the absolute thickness determined by XRR, with the differences presumably arising from the assumptions used to simplify the ESCA analysis. Since λ_e = 15 Å provides better agreement for the thinner overcoat thickness in which we are more interested, we will use the ESCA thicknesses determined with this value of λ_e for our further analysis.

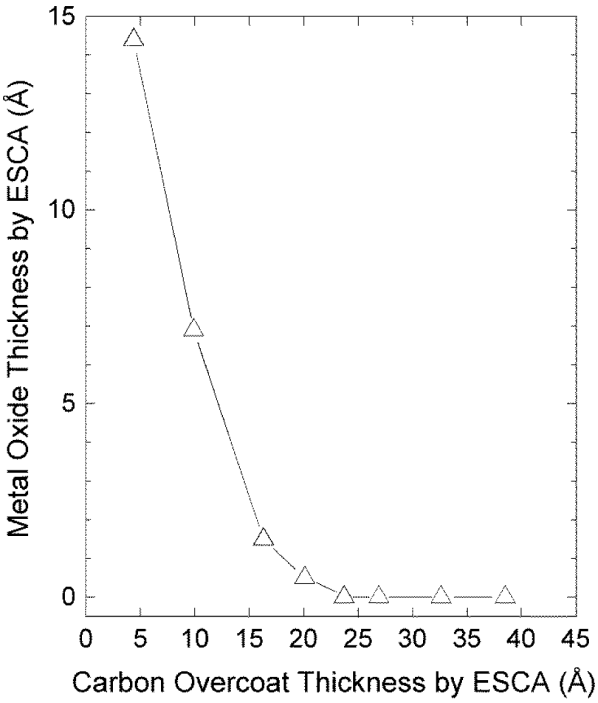

Fig. 7. Thickness of the metal oxide layer as function of CNx overcoat thickness, both determined by ESCA.

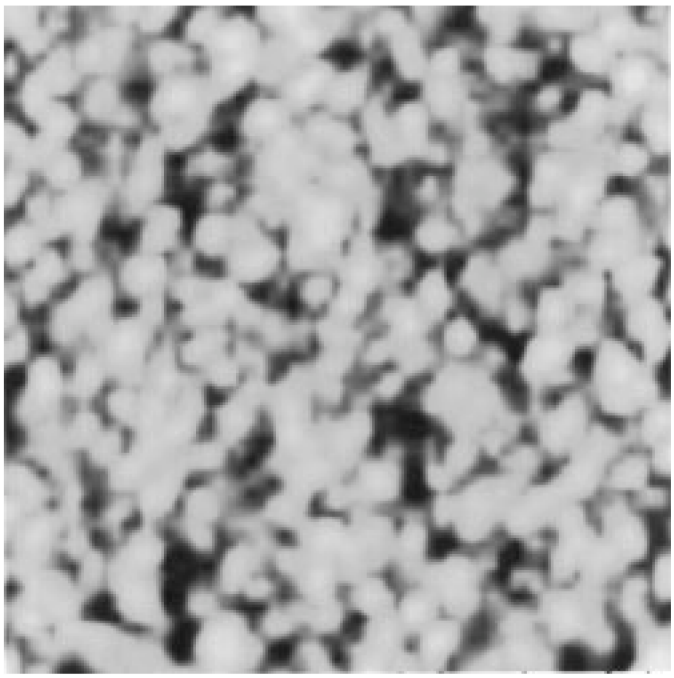

Fig. 8. AFM topography image of a 0.5 × 0.5 μm area of a disk surface with 12 Å (ESCA thickness) of CNx overcoat. The maximun height changes from dark to bright is 40 Å.

B. Determination of Overcoat Coverage by ESCA

As mentioned earlier, when the CNx films are thinner than 20 Å, metal oxide peaks are readily apparent in the ESCA spectra. The formation of an oxide layer indicates that the CNx overcoat is not completely covering the magnetic layer, as oxygen from the air is able to diffuse through these very thin overcoats and react with the metal atoms in the underlying magnetic layer. The disks had been stored in laboratory air (22°C, 20–60% relative humidity) for several months prior to the ESCA measurements. Assuming that metal oxide layer is at the magnetic layer/CNx overcoat interface (Fig. 5) and using the single-mean-free path model, we can determine an ESCA thickness for the oxide and other layers.

In Fig. 7, we plot the metal oxide layer thickness as a function CNx overcoat thickness, both determined by ESCA. The residual oxygen, which is readily distinguishable in ESCA from the oxide, corresponds to 1–2 Å thickness on the surface of the carbon overcoat. While coverage of a film can be characterized in many possible ways, we defined complete coverage of the CNx overcoat on the magnetic layer to be when the metal oxide layer is less than 1 Å thick. Several other ESCA studies [8], [9] have also observed that a 20 Å carbon film provides complete coverage by this definition. 20 Å may represent the thinnest possible overcoat achievable by today's sputtering deposition processes on a smooth surface that provides complete coverage. Protection against wear and corrosion may occur at different minimun thickness.

C. Disk Surface Topography

Fig. 8 shows an AFM image of a disk surface with 12 Å (ESCA thickness) of CNx overcoat. We have the following general observations from our AFM images of these surfaces:

TABLE I
XRR AND AFM SURFACE ROUGHNESS

CNx ESCA Thickness (Å)	XRR Glass/Mag. σ (Å)	XRR Mag./CNx σ (Å)	XRR CNx/air σ (Å)	AFM CNx/air σ (Å)
12	6	9.7	7.8	6.3
24	5.8	8.7	8.6	6.7
35	6.7	10.9	8.7	-
37	5	9.7	9.9	6.2
44	7	10	11.2	7.6

- The lateral dimensions of features observed for disks with magnetic layers and overcoats are the same as for the bare glass substrates. This indicates that the various layers in the thin film structure conformally cover the glass substrate and each other. Off-specular diffuse XRR shows oscillations at the same Q as the specular XRR, also indicating conformal roughness.
- For disks with an incomplete coverage of the CNx overcoat, like that shown in Fig. 8, we see no evidence of islands of either the CNx overcoat or the metal oxide. This indicates that, while the CNx overcoat coverage is incomplete, it is porous rather than discontinuous.
- The rms roughness σ increases with increasing overcoat thickness. Table I shows how the AFM roughness compares with roughness of the various interfaces determined by XRR.

From the table, one sees that both XRR and AFM rms roughness of the CNx/air interface increase with increasing thickness. The XRR roughness is larger than the AFM roughness as XRR samples over a larger lateral range: 1 Å to 2 μm for

XRR versus 80 Å to 2 μm for our AFM images. Consequently, XRR is able to measure roughness at shorter lateral length scales than AFM. The larger change in roughness observed by XRR with increasing overcoat thickness compared with AFM indicates that most of the increase in surface roughness is occurring at the shorter lateral length scales (<80 Å).

IV. Conclusion

The combination of XRR, ESCA, and AFM provides a thorough description of the structural parameters of ultra-thin CNx overcoats on magnetic recording disks.

- XRR measures absolutely the thickness, density, and roughness of the films if deposited on very smooth substrates and with a simple film structure.
- ESCA, if calibrated by XRR, can be used to determine overcoat thickness. ESCA can also be used to determine the overcoat coverage by monitoring the oxidation of the underlying magnetic layer. We find that the CNx overcoat coverage becomes incomplete when its thickness is less than 20 Å.
- AFM maps out topography variations. These maps show no evidence of CNx islands when the CNx overcoat coverage is incomplete. Also, even though the surfaces are very smooth ($\leq$11 Å rms roughness), the roughness increases with increasing overcoat thickness.

References

[1] M. F. Toney, C. M. Mate, and D. Pocker, *IEEE Trans. Magn.,*, vol. 34, pp. 1774–1776, July 1998.
[2] M. F. Toney, C. M. Mate, K. A. Leach, and D. Pocker, J.Colloid Interface Sci., submitted for publication.
[3] T. P. Russell, *Mater. Sci. Reports*, vol. 5, p. 5, 1990.
[4] M. F. Toney and C. Thompson, *J. Chem. Phys.*, vol. 92, p. 3781, 1990.
[5] A. Munkholm, S. Brennan, and E. C. Carr, *J. Appl. Phys.*, vol. 82, p. 2944, 1997.
[6] M. Born and E. Wolf, *Principles of Optics*. Oxford: Pergamon Press, 1970.
[7] D. Pocker, unpublished.
[8] B. Zhang, J. Ying, and B. Wei, *Data Storage Magazine*, pp. 49–52, Jan. 1998.
[9] M. K. Puchert, P. Y. Timbrell, R. N. Lamb, and D. R. McKenzie, *J. Vac. Sci. Technol.*, vol. A12, p. 727, 1994.